ECS Transactions, 50 (2) 1887-1893 (2012)
10.1149/05002.1887ecst ©The Electrochemical Society

Nitrogen-doped Graphene as an Active Electrocatalyst for Oxygen Reduction Reaction

D. Lee[a], A. Yu[a], and Z. Chen[a]

[a] Department of Chemical Engineering, Waterloo Institute of Nanotechnology, Waterloo Institute of Sustainable Energy, University of Waterloo, Waterloo, Ontario N2L 3G1, Canada, zhwchen@uwaterloo.ca

Nitrogen-doped graphene (NG) sheets are synthesized by thermal reduction and ammonia treatment of graphene oxide (GO). Scanning electron microscopy has revealed a voile-like morphology of NG sheets, which highly contrasts from the stacked layers observed with GO. X-ray photoelectron spectroscopy has verified successful nitrogen-doping of NG sheets, and Raman spectroscopy has confirmed a higher degree of deformation in NG sheets due to the incorporation of heterogeneous nitrogen atoms. To evaluate NG sheets as a highly active oxygen reduction reaction (ORR) electrocatalyst, half-cell electrochemical testing has been employed using rotating disk electrode (RDE) in an alkaline aqueous electrolyte. NG sheets demonstrate a pseudo four-electron pathway O_2 reduction, and a comparable ORR performance to that of a commercial carbon supported platinum (Pt/C) catalyst. This excellent ORR activity of NG sheets is most likely due to the active sites created by nitrogen-doping in the graphene sheets.

Introduction

A highly active electrocatalyst for oxygen reduction reaction (ORR) is important in the development of efficient fuel cells and metal-air batteries. Precious metal-based electrocatalysts such as platinum and palladium supported on carbon have been traditionally used to achieve efficient ORR (1-3). However, it is well-known in the literature that the ORR kinetics of these catalysts are still sluggish, and the catalyst becomes unstable upon extended cycling (4). Furthermore, with the price of precious metals continuing to rise, devices that use these catalysts are practically not feasible and are very difficult to commercialize. To replace these electrocatalysts, the scientific community have turned their attention to the development of non-precious metal-based catalysts as well as metal-free carbon-based catalysts. Previous reports show that these new catalysts are not only affordable, but also demonstrate excellent ORR activities (5-9). Amongst the new catalysts, graphene-based materials have risen as one of the most promising materials as graphene exhibits very interesting and useful properties such as very large surface area, high electrical conductivity, and thermal/chemical stability (10-13). Recently, nitrogen-doped graphene have been reported in the literature as a highly active ORR electrocatalyst although the exact active site and the mechanism are still unknown (14-16).

In this report, we synthesize nitrogen-doped graphene (NG) sheets via thermal reduction and ammonia treatment to evaluate its performance as an electrocatalyst for ORR in an alkaline aqueous electrolyte. The starting material, graphene oxide (GO), synthesized by the modified Hummers' method is exposed to an elevated temperature of 1000 ^{o}C with a flow of NH_3 using a horizontal tube furnace to produce NG. The oxygen functional groups of GO is removed by the thermal reduction to restore the sp^2 carbon network of graphene, and the NH_3 flow is used to introduce heterogeneous nitrogen dopants into the graphitic network to create ORR active sites. We evaluate the ORR activity of NG via half-cell testing using a rotating disk electrode (RDE), and compare with the ORR performance of the commercial carbon supported platinum (Pt/C) catalyst.

Experimental

Graphene oxide (GO) Synthesis

The synthesis of GO is carried out by the modified Hummers' method using natural graphite flakes (17). In a typical synthesis, 2 g of graphite flakes is added to 46 mL of concentrated sulphuric acid and stirred overnight. The mixture is put into an ice bath then 6 g of potassium permanganate is added under stirring. The ice bath is removed, and the mixture is stirred for one hour in ambient conditions. Next, 92 mL of distilled de-ionized (DDI) water is added drop-wise and stirred for another 30 minutes. Then, 280 mL of warm DDI water and 40 mL of 30 % H_2O_2 are added in sequence under stirring. The brown mixture is filtered and washed with 3 L of 5 % HCl solution, then centrifuged five times at 4000 rpm for 10 minutes. The mixture is collected and dried at room temperature.

Nitrogen-doped graphene (NG) Synthesis

In a typical synthesis of NG, 100 mg of GO is heated at 1000 ^{o}C using a horizontal tube furnace for 10 minutes with a mixed flow of 50 sccm of Ar and 50 sccm of NH_3. Then the furnace is turned off and cooled naturally under 100 sccm of Ar. After the furnace temperature is below 20 ^{o}C, the final product is collected from the tube.

Three-electrode half-cell test

Ring disk electrode (RDE) voltammetry is employed using a three-electrode electrochemical cell to evaluate the ORR activity of NG sheets in an alkaline aqueous electrolyte (0.1 M KOH). A potentiostat (Pine Instrument Co., AFCBP-1) and a rotation speed controller (Pine Instrument Co., AFMSRCE) are used for RDE voltammetry. All RDE voltammetry are performed at room temperature using a saturated calomel electrode (SCE) as a reference electrode, but the results presented in this report are converted to reversible hydrogen electrode (RHE). A platinum wire is utilized as a commonly used counter electrode (7, 8, 18). A glassy carbon electrode (5 mm OD) coated with 20 uL of 4 mg mL^{-1} suspension made by mixing NG sheets and a solution of 0.5 wt% Nafion in ethanol is used as a working electrode. ORR curves were recorded from -1.0 to 0.05 V at a scan rate of 10 mV s^{-1} with O_2-saturated electrolyte under various electrode rotation speeds (100, 400, 900, 1600 rpm). The ORR polarization curves were background

corrected by subtracting the currents obtained under the same testing conditions in Ar-electrolyte.

Koutechý-Levich plot and the number of electrons transferred (*n*) in ORR

Koutechý-Levich (K-L) equation relates the observed current density (j) with the kinetic current density (j_K) and limiting current density (j_L) as the following.

$$1 / j = 1 / j_K + 1 / j_L \quad [1]$$

The number of electrons transferred per O_2 molecule, *n*, is calculated from the following K-L equation,

$$j_L = 0.2 * n * F * D_o^{2/3} * \nu^{-1/6} * C_o * \omega^{1/2} \quad [2]$$

In the above equation, j_L is the limiting current density, F is the Faraday constant (96 485 C mol^{-1}), D_o is the diffusion coefficient of O_2 (1.9×10^{-5} cm^2 s^{-1}) in 0.1 M KOH, υ is the kinematic viscosity of 0.1 M KOH (0.01 cm^2 s^{-1}), and C_o is the concentration of O_2 in the electrolyte (1.1×10^{-6} mol cm^{-3}) (19).

Results and Discussion

The morphology of NG revealed by scanning electron microscopy (SEM) shows a voile-like structure of graphene sheets (Figure 1). The change in the morphology to NG sheets from GO is clearly observed as the micrograph of GO shows highly layered structure of the graphene sheets (Figure 1, Inset). The voile-like structure is consistent with previously reported results, confirming successful synthesis of NG sheets (16, 20).

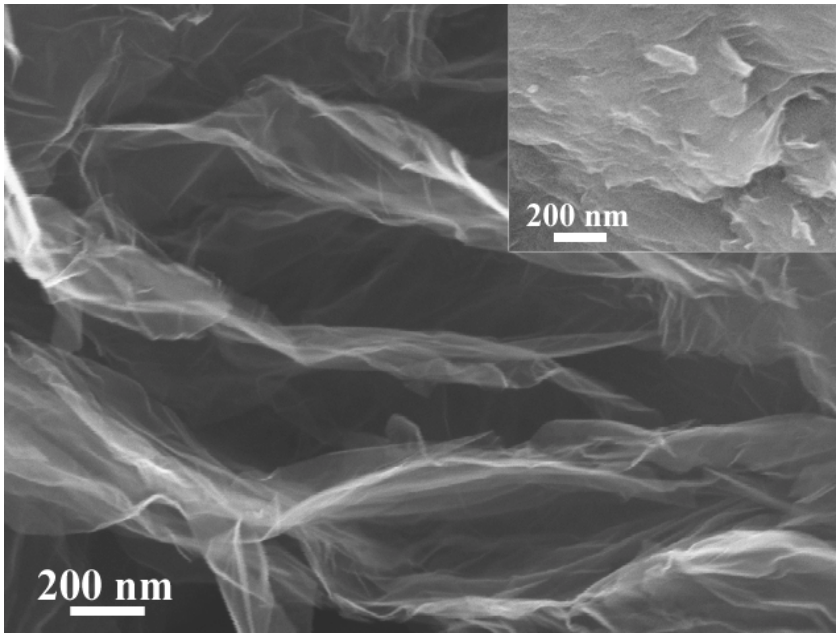

Figure 1. SEM image showing voile-like morphology of NG. Inset, SEM image of layered structure of GO sheets prior to the NG synthesis.

X-ray photoelectron spectroscopy (XPS) is employed to characterize the nitrogen content of NG sheets, and the distribution of nitrogen atoms into different species (Figure 2a). From the full XPS survey of NG sheets, the peak that corresponds to nitrogen is clearly observed, which is indicative of successful doping of heterogeneous nitrogen atoms into the graphitic network. The de-convolution of high-resolution N1 s peak is carried out to obtain ca. 5.2 atomic percent of nitrogen with a distribution of species into pyridinic, pyrrolic, and quaternary nitrogen species (Table I) (21, 22).

TABLE I. Atomic percent of nitrogen content and its distribution into different species after de-convolution of high resolution N1 s peak.

Sample Name	N content, at %	Pyridinic N, at %	Pyrrolic N, at %	Quaternary N, at %
NG	5.2	2.6	1.2	1.4

Raman spectroscopy is employed to characterize the degree of structural deformation caused by the introduction of nitrogen atoms into the sheets of NG (Figure 2b). The D and G bands of both NG and GO are observed at 1350 cm^{-1} and 1590 cm^{-1}, respectively. A higher value of I_D/I_G, the ratio of the intensities of the two bands, is an indication of a larger degree of deformation as the D band is characteristic of disorder in the graphitic plane, whereas the G band is characteristic of the sp^2 carbon network in graphene (23). Hence, a higher I_D/I_G ratio of 1.12 observed with NG compared to 0.97 for GO is indicative of a larger degree of deformation in NG sheets due to the incorporation of heterogeneous nitrogen species.

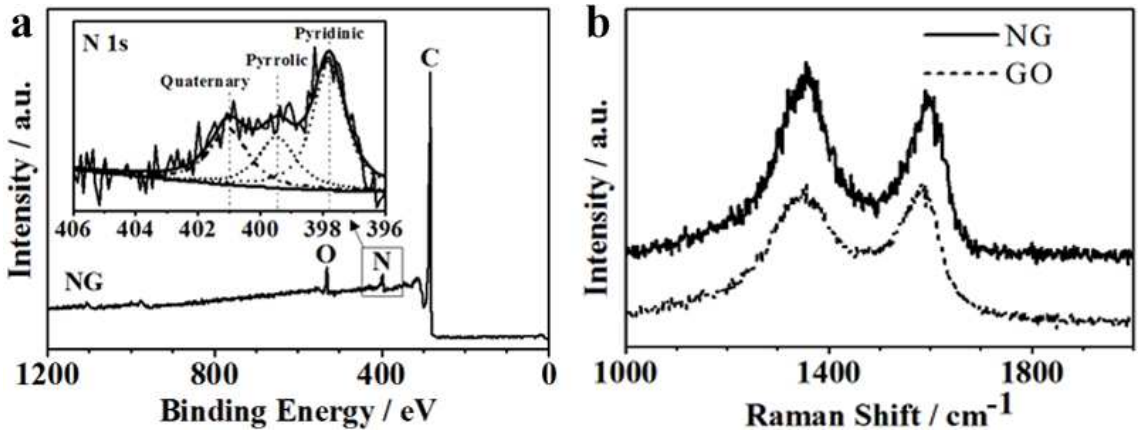

Figure 2. a, Full XPS survey of NG. Inset, De-convolution of high resolution N 1s XPS spectrum into pyridinic, pyrrolic, and quaternary nitrogen species. b, Raman spectra of NG and GO.

The half-cell testing is employed using rotating disk electrode (RDE) to evaluate the ORR activity of NG in an alkaline aqueous electrolyte. The ORR polarization curves of NG at various rotation rates show well defined kinetics- and diffusion-limited regions (Figure 3a). The Koutecký-Levich plot is used to calculate the number of electrons transferred, *n*, per O_2 molecule in ORR at potentials of 0.30 V, 0.35 V, 0.40 V, and 0.45 V (vs. RHE) according to the equations outlined in the experimental section (Figure 3b).

The obtained values of *n* are very close four, which is indicative of the ORR occurring via a pseudo four-electron reduction pathway ($O_2 + 2H_2O + 4e^- \rightarrow 4OH^-$) (Table II). The four-electron reduction pathway observed in NG is highly desirable in an efficient electrocatalyst as the two-electron pathway produces corrosive peroxides that degrade the catalyst.

TABLE II. Number of electrons transferred during ORR at various potentials.

Potential vs. RHE	Number of electrons transferred (*n*)
0.30 V	4.0
0.35 V	4.0
0.40 V	3.9
0.45 V	3.9

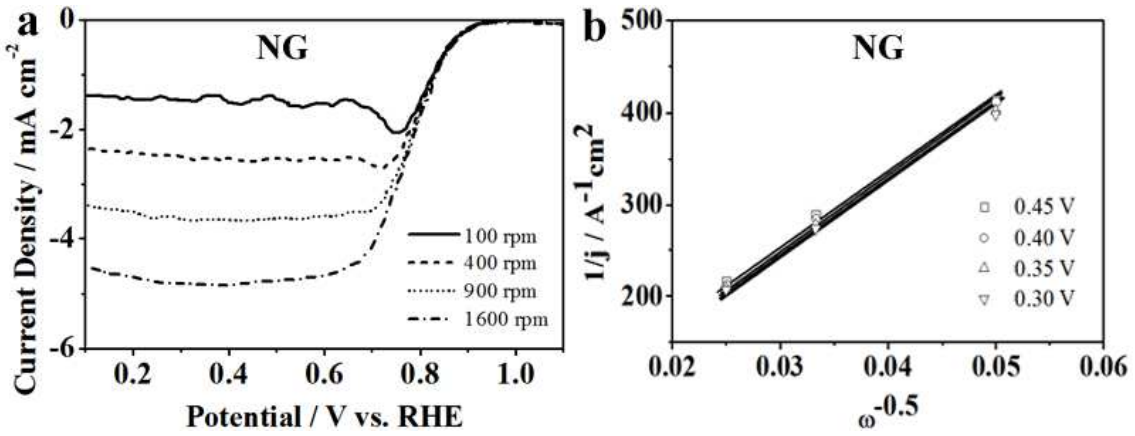

Figure 3. a, ORR polarization curves of NG at various rotation rates. b, Koutecký-Levich plot of NG at potentials 0.30 V, 0.35 V, 0.40 V, and 0.45 V (vs. RHE).

To confirm the excellent ORR activity of NG, its performance is compared to that of Pt/C (Figure 4a). From the ORR polarization curve of NG sheets obtained at the rotation rate of 1600 rpm, the onset potential of 0.950 V (vs. RHE) and the half-wave potential of 0.794 V (vs. RHE) are obtained, which are slightly lower but comparable to those obtained with Pt/C (0.969 V (vs. RHE) and 0.829 V (vs. RHE), respectively) (Figure 4a). In addition, the Tafel slope, an indication of ORR kinetics, is calculated to be 81 mV/decade for NG, which is very similar to that of Pt/C (79 mV/decade) to show that their performance are comparable (Figure 4b).

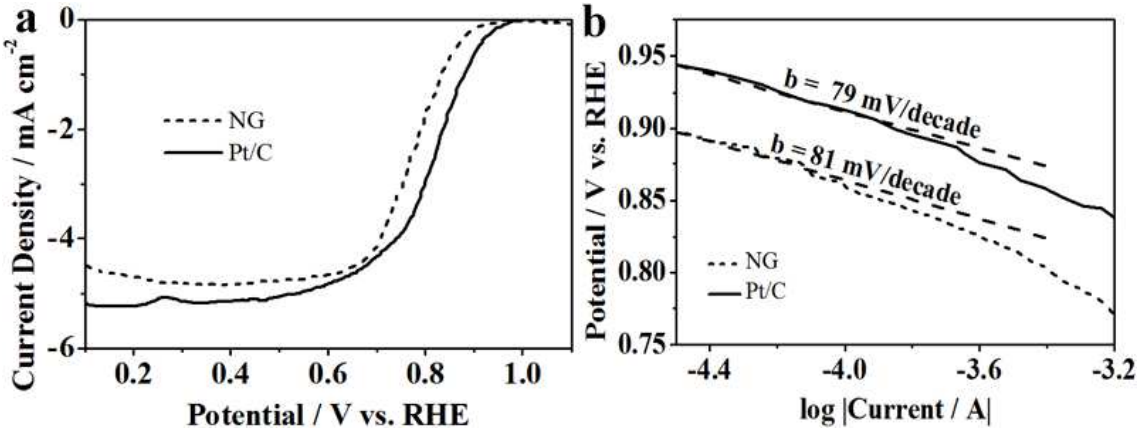

Figure 4. a, ORR polarization curves of NG and Pt/C obtained by RDE voltammetry at a rotation rate of 1600 rpm. b, Tafel plot of NG and Pt/C in the low current density region.

In conclusion, highly ORR active electrocatalyst is synthesized by thermal reduction and ammonia treatment. The voile-like graphene morphology of NG is confirmed by SEM, and the nitrogen content is determined to be ca. 5.2 atomic percent after the de-convolution of the high resolution nitrogen XPS peak. The analysis of the Koutecký-Levich slope shows a pseudo four-electron reduction pathway for NG. Compared to the state-of-the-art commercial Pt/C catalyst, NG shows a comparable ORR activity with only slightly lower values of onset and half-wave potentials. This excellent ORR activity of NG sheets is most likely due to the active sites created by the heterogeneous nitrogen atoms in the graphitic network.

Acknowledgments

This research was supported by the Natural Sciences and Engineering Research Council of Canada (NSERC) through grants to Dr. Zhongwei Chen, and the University of Waterloo.

References

1. S. Guo, S. Dong and E. Wang, *ACS Nano*, **4**, 1 (2009).
2. G. Kim and S.H. Jhi, *ACS Nano*, **5**, 2 (2011).
3. D.C. Higgins, D. Meza and Z. Chen, *The Journal of Physical Chemistry C*, **114**, 50 (2010).
4. K. Gong, F. Du, Z. Xia, M. Durstock and L. Dai, *Science*, **323**, 5915 (2009).
5. J.-Y. Choi, D. Higgins and Z. Chen, *Journal of The Electrochemical Society*, **159**, 1 (2012).
6. Z. Chen, D. Higgins, A. Yu, L. Zhang and J. Zhang, *Energy & Environmental Science*, **4**, 9 (2011).
7. S. Zhu, Z. Chen, B. Li, D. Higgins, H. Wang, H. Li and Z. Chen, *Electrochimica Acta*, **56**, 14 (2011).
8. Z. Chen, A. Yu, D. Higgins, H. Li, H. Wang and Z. Chen, *Nano Letters*, **12**, 4 (2012).
9. X. Li, H. Wang, J.T. Robinson, H. Sanchez, G. Diankov and H. Dai, *Journal of the American Chemical Society*, **131**, 43 (2009).
10. A.K. Geim and K.S. Novoselov, *Nat Mater*, **6**, 3 (2007).
11. S. Yang, X. Feng, X. Wang and K. Müllen, *Angewandte Chemie International Edition*, **50**, 23 (2011).
12. H. Wang, Y. Yang, Y. Liang, J.T. Robinson, Y. Li, A. Jackson, Y. Cui and H. Dai, *Nano Letters*, **11**, 7 (2011).
13. G. Yu, L. Hu, M. Vosgueritchian, H. Wang, X. Xie, J.R. McDonough, X. Cui, Y. Cui and Z. Bao, *Nano Letters*, **11**, 7 (2011).
14. L. Qu, Y. Liu, J.-B. Baek and L. Dai, *ACS Nano*, **4**, 3 (2010).
15. K.R. Lee, K.U. Lee, J.W. Lee, B.T. Ahn and S.I. Woo, *Electrochemistry Communications*, **12**, 8 (2010).

16. D. Geng, Y. Chen, Y. Chen, Y. Li, R. Li, X. Sun, S. Ye and S. Knights, *Energy & Environmental Science*, **4**, 3 (2011).
17. W.S. Hummers and R.E. Offeman, *Journal of the American Chemical Society*, **80**, 6 (1958).
18. Z. Chen, A. Yu, R. Ahmed, H. Wang, H. Li and Z. Chen, *Electrochimica Acta*, **69**, 0 (2012).
19. G. Wu, G. Cui, D. Li, P.-K. Shen and N. Li, *Journal of Materials Chemistry*, **19**, 36 (2009).
20. M.J. McAllister, J.-L. Li, D.H. Adamson, H.C. Schniepp, A.A. Abdala, J. Liu, M. Herrera-Alonso, D.L. Milius, R. Car, R.K. Prud'homme and I.A. Aksay, *Chemistry of Materials*, **19**, 18 (2007).
21. F.d.r. Jaouen, J. Herranz, M. Lefèvre, J.-P. Dodelet, U.I. Kramm, I. Herrmann, P. Bogdanoff, J. Maruyama, T. Nagaoka, A. Garsuch, J.R. Dahn, T. Olson, S. Pylypenko, P. Atanassov and E.A. Ustinov, *ACS Applied Materials & Interfaces*, **1**, 8 (2009).
22. P.H. Matter, L. Zhang and U.S. Ozkan, *Journal of Catalysis*, **239**, 1 (2006).
23. D. Geng, S. Yang, Y. Zhang, J. Yang, J. Liu, R. Li, T.-K. Sham, X. Sun, S. Ye and S. Knights, *Applied Surface Science*, **257**, 21 (2011).